On primary energy reconstruction for IceTop

Samvel Ter-Antonyan and Ali Fazely
Southern University, Baton Rouge, LA

Abstract. **Primary energy reconstruction method is presented for the ICETOP experiment. Results are obtained on the basis of CORSIKA EAS simulations taking into account the detector response and shower reconstruction uncertainties. Comparison of our results with ICETOP data published in 2008-2009 has disclosed certain unaccountable inconsistencies and needs further discussions in the frames of the ICETOP Cosmic Ray group [1].**

MOTIVATION

Our report "Primary energy reconstruction for IceTop Array" at the Madison-2009 ICECUBE workshop indicated that there is a disagreement between ICETOP's and ours $E_0 - E_1$ scatter plots for proton and Iron primary particles. Our results point towards a slow convergence of proton and Iron $E_0 - E_1$ data in the region of 10^8 GeV energies, whereas the ICETOP proton and Iron data had an explicit intersection in the region of 10^7 GeV.

Looking through the new data presented by the cosmic ray group at 2009 ICRC we noted that the intersection behavior of ICETOP's proton and Iron $E_0 - E_1$ scatter plots remained practically the same.

To figure out this problem, we re-simulated the ICETOP experiment from shower simulation up to the reconstruction of primary energy considering practically all existing sources of fluctuations and uncertainties.

The sections below are organized as follows.

1. Energy reconstruction accuracy and biases.
2. Tank-to-tank and tank-to-fit fluctuations.
3. Reconstruction of shower parameters.
4. Conclusion
5. Proposal

Appendix I: CORSIKA steering cards.
Appendix II: Tank calibration (definition of VEM).
Appendix III: Fluctuations of DOM.

I. PRIMARY ENERGY RECONSTRUCTION, ACCURACIES AND BIASES.

A. Primary energy evaluation

Primary energy evaluation method was tested using the configuration of tanks (ICETOP 2009) presented in Fig. 1 (filled circles) and CORSIKA simulated shower samples (doted symbols) in the energy range $5{\cdot}10^5 - 10^8$ GeV and energy spectral index $\gamma = -1.5$. The number of simulated events was equal to $N_A = 1000$ for each of $A \equiv H.He, O, Fe$ primary nuclei (for corresponding CORSIKA steering cards see Appendix I).

[1]Corresponding author: samvel_terantonyan@subr.edu

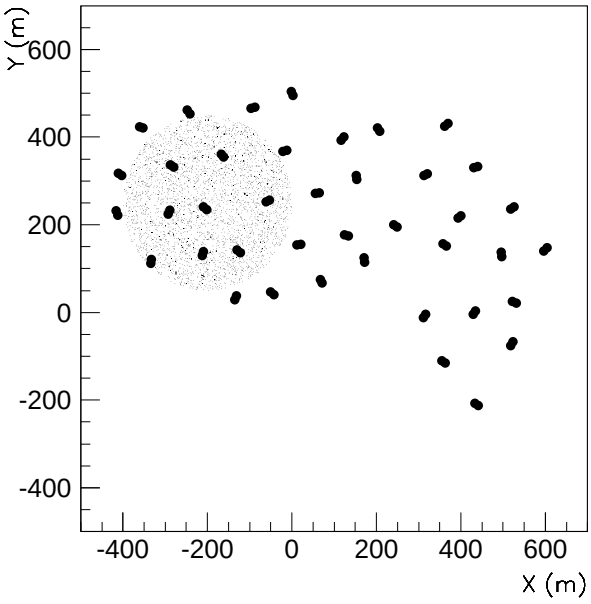

Fig. 1. ICETOP tank configuration (filled circles) and distribution of 4×1000 CORSIKA simulated shower core x, y coordinates.

We estimated the energy of primary nuclei ($\ln E_0$) according to log-linear approximation

$$\ln\left(\frac{E_1}{1GeV}\right) = a + \frac{b}{\cos\theta} + c \ln n_{eq} \qquad (1)$$

where $n_{eq} = S_{125}/\text{VEM}$ is an evaluation of the average number of equivalent particles in the effective area of the ICETOP tank at the reference ($R_{ref} = 125$m) radius from the shower core, VEM is the average number of photoelectrons produced by the single Vertical Equivalent Muon (for details see Appendix II) accepted in the ICETOP experiment, and θ is the shower zenith angle.

Parameters $a = 12.47 \pm 0.05$, $b = 1.14 \pm 0.05$, $c = 1.037 \pm 0.002$ are derived from the minimization of the χ^2 function

$$\chi^2 = \sum_A \sum_{i=1}^{N_A} = \frac{(\ln E_{0,i} - \ln E_{1,i})^2}{\sigma^2(\ln E_1)} \qquad (2)$$

where the first sum involves 4 kinds of primary nuclei $A \equiv H, He, O, Fe$, $N_A = 1000$ is the number of simulated showers with E_0 "true" primary energies and E_1 reconstructed energies according to (1).
The energy estimation errors $\sigma(E_1)$

$$\sigma(\ln E) = \sqrt{\frac{4 \cdot 10^4 GeV}{E}} + 0.03 \qquad (3)$$

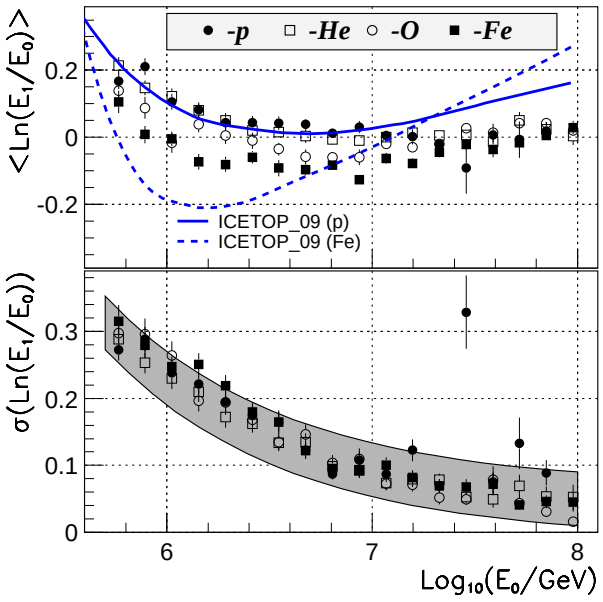

Fig. 2. Primary energy evaluation biases (top panel) and errors (lower panel) for $A \equiv p, He, O, Fe$ nuclei. Shaded area steams from (3) with uncertainty $\pm 5\%$.

were determined iteratively with uncertainty $\Delta_\sigma = 0.05$ for $\chi^2_{\min}/n_{d.f.} \simeq 1.48$.

The energy evaluation biases $\langle \ln E_1 - \ln E_0 \rangle$ (top panel) and corresponding errors σ (lower panel) are presented in Fig. 2 (symbols). The blue lines represent ICETOP 2009 results [1]. Corresponding $E_0 - E_1$ scatter plots are shown in Fig. 3.

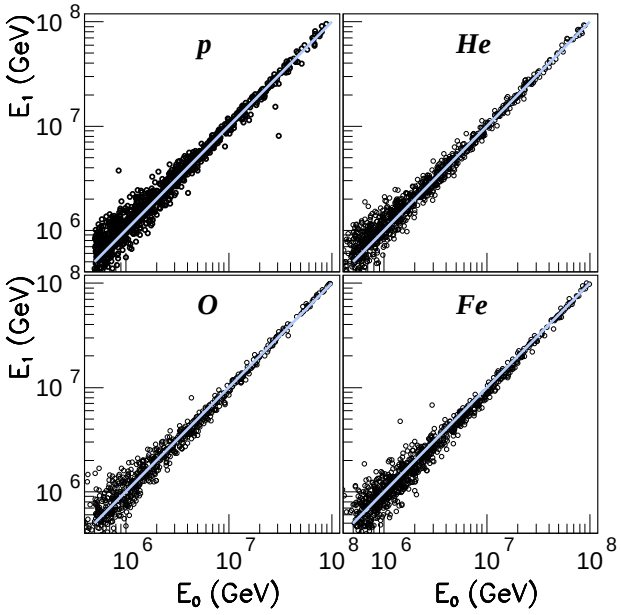

Fig. 3. True (E_0) and estimated (E_1) energy distributions for 4 kinds of primary nuclei. White lines are $E_0 = E_1$ dependencies.

B. Discussion (Section I)

As it is seen from Figs 2,3 (symbols), **the biases of energy reconstruction slowly converge in the energy region $\sim 10^8$ GeV, whereas the ICETOP_09 results (blue lines) show more complicated behavior with intersection feature**.

Here, it is necessary to note that the uncertainty of the inverse problem solution for all-particle primary energy spectrum depends significantly on biases $\propto \langle E_1/E_0 \rangle^{\gamma-1}$ with energy spectral index $\gamma \simeq 3$ and relative errors $\propto \exp([(\gamma-1)\sigma_E]^2/2)$, [2].

Hence, any rapid change of these parameters can imitate the spectral knee or vice versa, smooth out the existing knee (see [2] for details).

The events with underestimated energies (Fig. 3, p, $E_0 > 10^7$ GeV) correspond to diffractive interactions (or interactions with small inelasticity) of primary protons and are unavoidable in the ICETOP experiment. However, these events will not change the all-particle energy spectrum due to very steep (E_A^{-3}) expected energy spectra and the corresponding bump in Fig. 2 (lower panel) at energy $\sim 3 \cdot 10^7$ GeV can be ignored.

II. Tank-to-tank and tank-to-fit fluctuations

The reason for observed disagreement between ICETOP_09 and our results (top panel of Fig. 2) could be the differences of evaluation of $n_{eq} = S_{ref}/\text{VEM}$. Therefore, we studied tank-to-tank and tank-to-fit discrepancies for ICETOP tank configuration (Fig. 1). The results are presented in Figs 4,5.

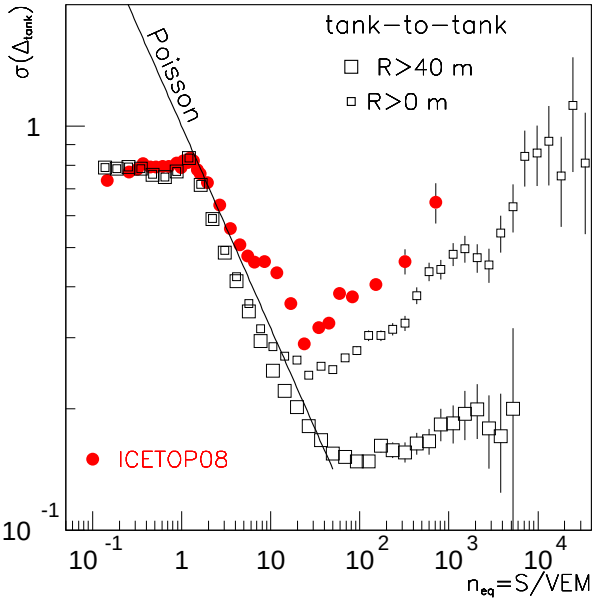

Fig. 4. Tank-to-tank fluctuations $\Delta_{tank} = \ln(n_{eq,i}/n_{eq,i+1})$, (reduced by a factor of $1/\sqrt{2}$) for $S_{\min} = 20$pe lower threshold of DOMs, condition of coincidence in the station, and $R > 100$m distances of stations from shower core.

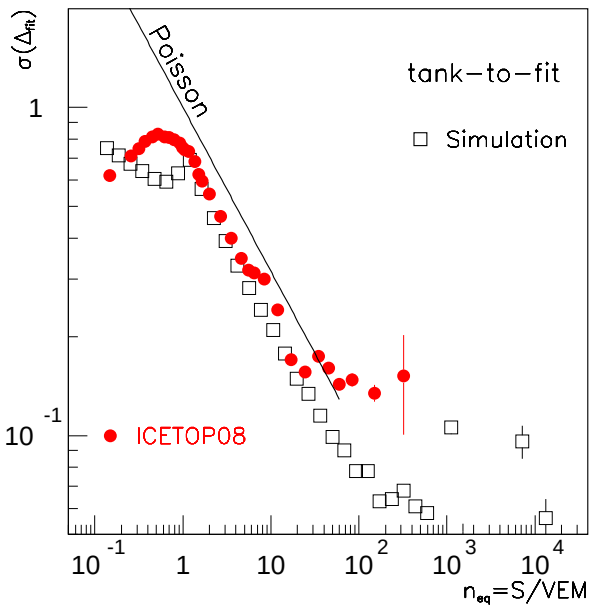

Fig. 5. Tank-to-fit fluctuations $\Delta_{fit} = \ln(n_{eq,i}/n_{eq,fit})$, for $S_{\min} = 1$pe lower threshold of DOMs.

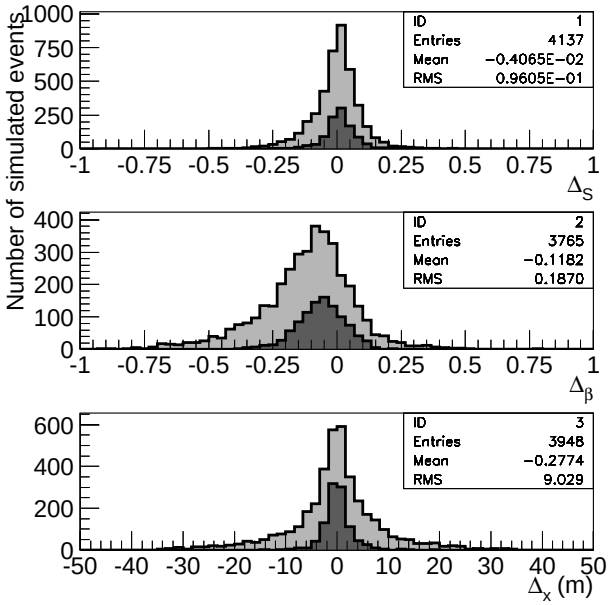

Fig. 6. Shower reconstruction error distributions for $\Delta_S = (\ln n_{eq})^* - \ln n_{eq}$ (upper panel), $\Delta_\beta = \beta^* - \beta$ (median panel) and $\Delta_x = x_0^* - x_0$ (lower panel). Black shaded histograms are the same distributions for energies $E_A > 5 \cdot 10^6$ GeV.

A. Discussion (Section II)

ICETOP description (approximations) of tank-signal fluctuations is a little bit farther from reality due to unavoidable **Poisson fluctuations** which have to equal to about $\sigma(\ln n_{eq}) \simeq 1$ in the region of $n_{eq} \simeq 1$. This conclusion is confirmed by independent investigations of DOM's fluctuation presented in Appendix III below.

III. Reconstruction of shower parameters S_{ref}, β, x_0, y_0

Reconstruction of shower parameters were carried out using simple 4-parametric $(S_{ref}, \beta, x_0, y_0)$ minimization of the χ^2 function

$$\chi^2 = \sum_{i=1}^{m>10} \frac{(\ln n_{eq,i} - \ln n_{eq,i,fit})^2}{\sigma^2(\ln n_{eq,i})} \qquad (4)$$

where $n_{eq,i,fit} = f(S_{ref}, \beta, R(x_0, y_0))$ is the corresponding double-logarithmic fit of the lateral distribution function accepted by the ICETOP group [1]. The minimization of expression (4) was performed by the FUMILI CERNLIB code.

The main complexity of minimization (4) is a dependence of σ_i on distance R_i, i.e. unknown coordinates (x_0, y_0). However, this dependence is negligible for the ICETOP experiment, where practically all stations are located at $R \gg 10$m from the shower core position (see Appendix III). Hence, we used $\sigma(\ln n_{eq}, R_{1,i})$ in (4) applying initial iteration values $(x_1, y_1$, see below) for the shower core coordinates.

In expression (4) we also used the trigger condition for stations $(S_i, S_{i+1} > 20$pe) and a shower trigger, $m > 10$ [1]. For the initial value of iteration (x_1, y_1) we used weighted average tank coordinates with weights $w_i = 1/S_i^2$, as opposed to the ICETOP weights $(1/S_i)$ [1].

To estimate the accuracy of the shower parameters reconstruction we used an analytical solution for the χ^2 minimization above at known coordinates (x_0, y_0) of shower core. The solution (estimation) for the shower parameter β is

$$\beta^* = -\frac{\sum \frac{1}{\sigma_i^2} \mathbf{L}S_i \mathbf{L}z_i + k \sum \frac{1}{\sigma_i^2} \mathbf{L_2}z_i \mathbf{L}z_i}{\sum \frac{1}{\sigma_i^2} (\mathbf{L}z_i)^2} \qquad (5)$$

where logarithmic operators $\mathbf{L}z_i = \ln z_i - \overline{\ln z_i}$ and $\mathbf{L}_2 z_i = \ln^2 z_i - \overline{\ln^2 z_i}$, and $z_i = \ln R_i/R_{ref}$.

The estimation of S_{ref} is derived from

$$\ln S_{ref}^* = \frac{\sum \frac{1}{\sigma_i^2} \ln S_i - \sum \frac{1}{\sigma_i^2} \ln \alpha_i}{\sum \frac{1}{\sigma_i^2}} \qquad (6)$$

where $\alpha_i = -\beta \ln z_i - k(\ln^2 z_i)$.

Reconstruction accuracies of showers $\ln S_{125}$ (upper panel), β (median panel) and x_0 (lower panel) parameters are presented in Fig. 6. Black shaded histograms correspond to higher primary energies $(E_0 > 5 \cdot 10^6$ GeV).

The observed bias $\langle \Delta_\beta \rangle \simeq -0.12$ for the reconstructed β parameter in Fig. 6 is due to 20pe lower thresholds of DOMs. The reconstruction errors for n_{eq} and x, y shower core coordinates are about 10% and 9m respectively and these values get better for higher primary energy.

The efficiency of reconstruction is well seen from Fig. 7 where contour plots represent the domains of 4000 "true" values of S_{125} and β derived from expressions

(5,6) for known x_0, y_0 coordinates. The dot symbols show the distribution of reconstructed S_{125} and β parameters of showers. Using the observed contour plots one can determine the boundary conditions for the derived shower parameters.

In Fig. 8 the examples of reconstructed lateral distribution functions ($n_{eq}(R|E,A)$) are presented (filled circle symbols) for primary proton (left panel) and Iron (right panel) nuclei with energies $E_A \equiv 5 \cdot 10^5$ (red), $5 \cdot 10^6$ (blue) and $5 \cdot 10^7$ GeV (black). The hollow square symbols represent the "measured" tank data. The corresponding shower zenith angles and $\chi^2/n_{d.f.}$ are shown as well. The average goodness-of-fit test for all simulated (Fig. 1) and reconstructed showers was equal to $\chi^2_{min}/n_{d.f.} \sim 1$

As it is seen from Fig. 8, the $\chi^2_{\min}/n_{d.f.}$ values of reconstructed showers are about ~ 1, which indicates the correctness of fluctuations $\sigma(\ln n_{eq})$ taken into account in the minimization (4) (for details see the Appendix III).

Unfortunately, we could not compare these results with the same ICETOP data. **It is interesting to make this comparison because the method applied above is significantly simpler than the one used by the ICETOP group**.

Also, analytic solutions (5,6) for $\ln S_{ref}$ and β shower parameters transform the 4-parametric minimization problem into 2-parametric (only x_0, y_0) problem, which improves the robustness of minimization (4) and is extremely important for the reconstruction of shower parameters at low energy region ($5 \cdot 10^4 - 5 \cdot 10^5$ GeV).

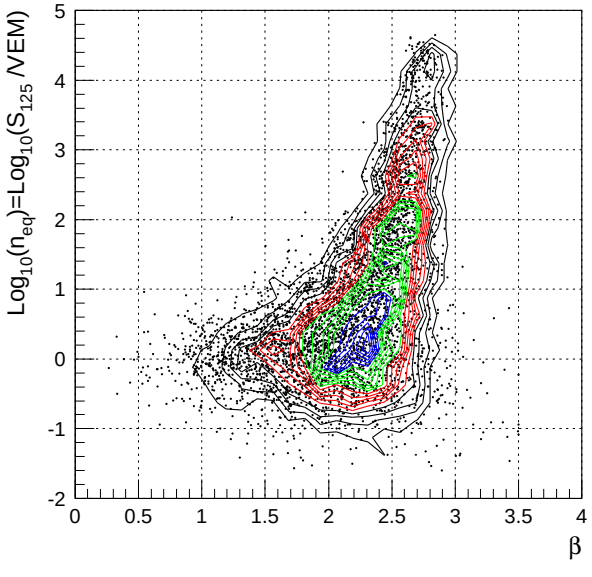

Fig. 7. "True" and reconstructed $\log_{10}(n_{eq}) - \beta$ scatter plot. The contour lines are domains of "true" values derived from expressions (5,6) and known x_0, y_0. Dot symbols are scatter plot for parameters of corresponding reconstructed showers.

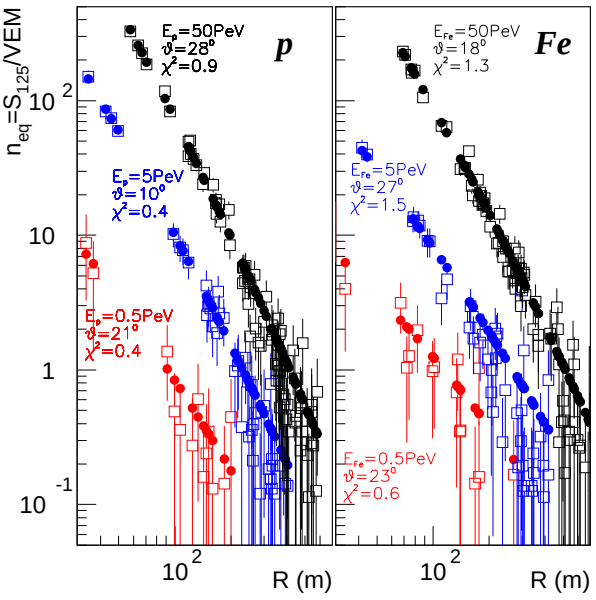

Fig. 8. Examples of reconstructed lateral distribution functions (filled circle symbols) for primary proton (left panel) and Iron (right panel) nuclei with energies $E_A \equiv 5 \cdot 10^5$ (red), $5 \cdot 10^6$ (blue) and $5 \cdot 10^7$ GeV (black). The hollow square symbols represent the "measured" tank data. Corresponding shower zenith angles and $\chi^2/n_{d.f.}$ are shown as well.

However, for briefness, we omit these details here.

IV. Conclusion

Expression (1) as first approximation is ready to be applied for the event-by-event evaluation of primary energy regardless of primary nuclei kind. We presume that increasing the simulated samples and accurately accounting for the ICETOP trigger conditions will improve the expected results.

The reconstruction of the all-particle energy spectrum has to be performed taking into account the existing biases and errors represented in Fig. 2 and expression (3) (see [2]). From this viewpoint, our results presented in Fig. 2 are more preferable as opposed to the ICETOP data from [1].

V. Proposal

Before the reconstruction of the all-particle energy spectrum it is interesting to study the so called "tank-particle" spectra. It is the $\partial f(E_A, R)/\partial n_{eq}$ spectra averaged for all tanks into a given $R_{\max}$ maximal radius from reconstructed shower cores and integrated over all primary particles and energies:

$$\frac{dF(R_{\max})}{dn_{eq}} = \sum_A \int \frac{d\Im}{dE_A} \left\langle \frac{\partial f(E_A, R)}{\partial n_{eq}} \right\rangle_{R<R_{\max}} dE_A. \quad (7)$$

Our analysis suggests, that these spectra slightly depend on the elemental composition and interaction model (QGSJET,SIBYLL), and strongly depend on the

all-particle energy spectrum and measurement errors.

In Fig. 9 the expected "tank-particle" spectra are presented for all simulated events from Fig. 1 and $R_{max} = 100$m and 500m respectively. The primary energy spectra $d\Im/dE_A$ for $A \equiv H, He, O, Fe$ primary particles were taken from [3] approved in $10^5 - 10^8$ GeV energy region.

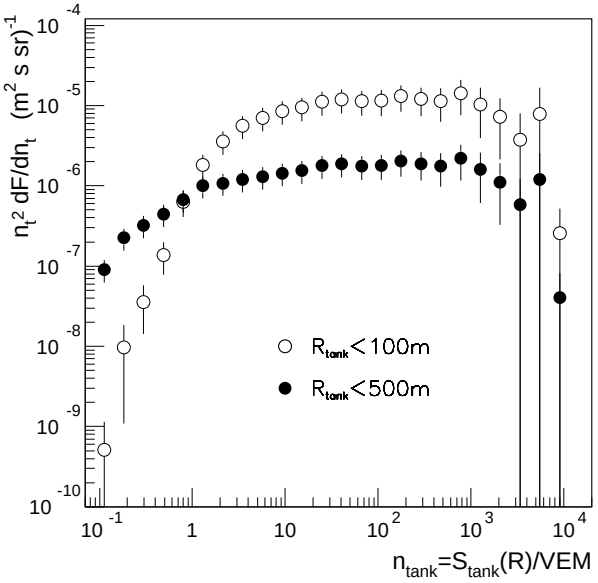

Fig. 9. "Tank-particle" spectra for two radii according to expression (7) (see Section 5 for details).

Appendix I: CORSIKA steering cards

EAS simulations were carried out for 4 primary nuclei (p, He, O, Fe) using ICETOP CORSIKA steering cards:

ESLOPE -1.5
ERANGE 0.5E6 1.0E8
THETAP 0.000 30.0
PHIP 0.000 360.0
SEED 102501 12 0
SEED 298373 98 0
ATMOD 12
OBSLEV 2835.E2
HADFLG 0 1 0 1 0 2
ECUTS 0.1 0.1 0.01 0.005
ELMFLG F T
MAGNET 16.59 -52.79

The primary energy range is $0.5 - 100$ PeV for $0 - 30^0$ zenith angular interval. The spectral index of simulation was -1.5 to provide reliable statistics for a high energy region.

Appendix II: Tank calibration (definition of VEM)

For the calibration of the tank we used CORSIKA simulations for primary H and He nuclei, into $0 - 60^0$ zenith angular interval and $10 - 10^3$ GeV energy range according to corresponding Biermann's energy spectra. The solar modulations term was neglected.

Each secondary particle (e, γ, μ) at the observation level of ICETOP passed through the tank independently and without failing at known (from CORSIKA) angular coordinates.

The (x, y) space coordinates were distributed uniformly within the extended $R < 1.6$m hypothetical upper cap of the tank. The average number of photoelectrons detected in the tank $S_{pe}(E_{e,\gamma,\mu})$ was computed from corresponding ICETOP(GEANT) simulated data [4] weighted proportionally to the computed length of the particle trajectory in the tank.

Cherenkov light fluctuations $\sigma_{\gamma,e}$ and σ_μ were free parameters and were estimated by comparing simulated photoelectron spectra with experimental ICETOP data (DOM21-64).

The additional source of fluctuations used in our simulations was the Poisson fluctuations of photoelectron numbers produced in a PMT.

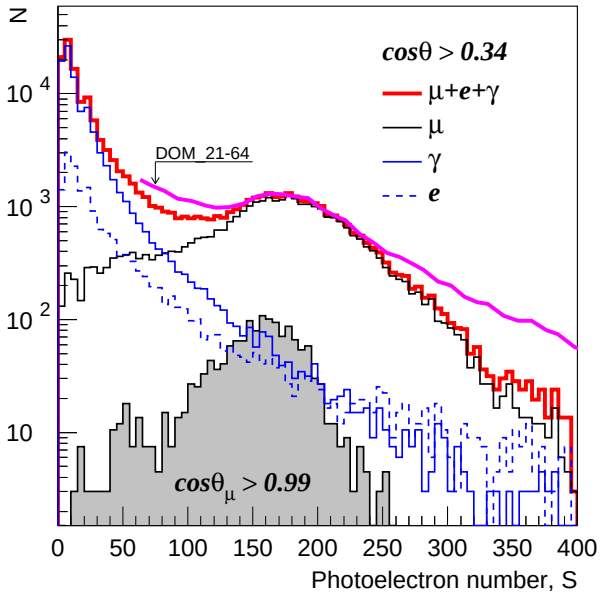

Fig. 10. Simulated (produced by the background γ, e, μ flux) and detected (ICETOP, DOM 21-64,2007) photoelectron (pe) spectra. Photoelectron spectrum produced by the vertical muon flux (shaded histogram) determines the corresponding photoelectron number, VEM= 175pe, for our simulation. Two free parameters, the fluctuations of Cherenkov light $\sigma_{\gamma,e} = 0.30 \pm 5$ from γ-quanta and electrons and $\sigma_\mu = 0.15 \pm 0.3$ from muons were estimated on the basis of agreement of summary spectrum (red histogram) with ICETOP data. The steep simulated spectrum for $S > 250$pe can be explained by the contribution of multiparticle passage through the tank which is not taken into account in our analysis.

The photoelectron spectra produced by simulated single background particles are presented in Fig. 10 in comparison with the ICETOP data.

APPENDIX III: FLUCTUATIONS OF DOM.

We studied shower fluctuations using the shower array presented in Fig. 11 with concentrically positioned 24 tanks for each of 10 radii: 10, 50, 100, 150, ..., 400, 500m.

Simulated showers had zero angular and space coordi-

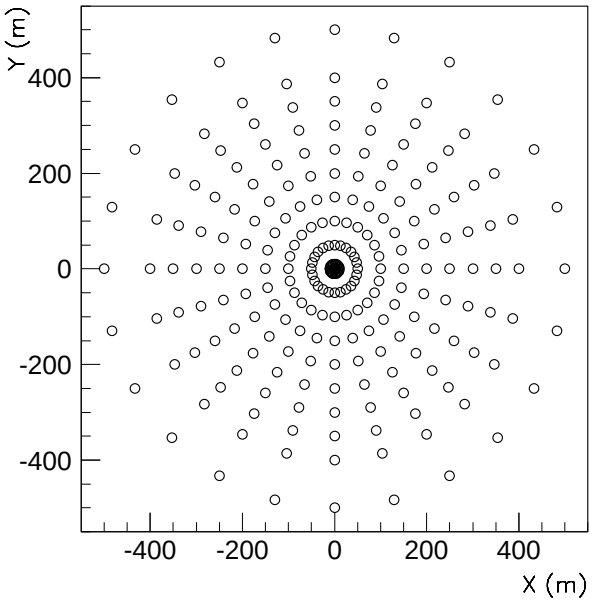

Fig. 11. Hypothetical shower array. The 24 tanks are located in each of the 10 concentric circles.

nates. The primary energy range was $5 \cdot 10^4 - 10^8$ GeV with -1.5 energy spectral index. Simulated samples contained 500 events for each of the primary $A \equiv H, He, O, Fe$ nuclei with energies $E_A > 5 \cdot 10^5$ GeV.

The obtained fluctuations $\sigma/n_{eq} \simeq \sigma(\ln n_{eq})$ of the observed effective number of equivalent particles depending on computed average number of particles $n_{eq} = S_R/\text{VEM}$ for different radii R are presented in Figs 12,13.

A. Discussion (Appendix III)

Figs 12,13 demonstrate that the shower fluctuation is significant only for radii $R \ll 50$ m. The drop of fluctuations for $n_{eq} \leq 1$ is completely explained by the lower threshold of a detected photoelectron number.

The fluctuations are practically Poissonian for radii $R > 50$ m and slightly depend on a primary nuclei kind and a zenith angle.

Results (from Figs. 4,5) point towards the existence of an additional $\sim 5\%$ systematic errors in the tank response.

The obtained values of fluctuations (Fig. 12) were tabulated in the 10×30 2-dimensional bins (10 radii and 30 bin for n_{eq}) and were used for the reconstruction of S_{125} (expression (4)).

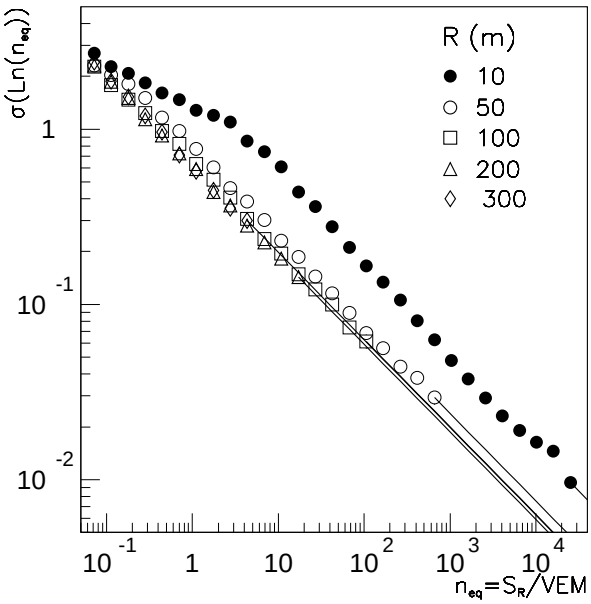

Fig. 12. Fluctuation of tank for different radii at photoelectron threshold $S_{\min} = 1$ (symbols). The lines are $1/\sqrt{n_{eq}}$ extrapolations of data normalized at the last (right) computed bins.

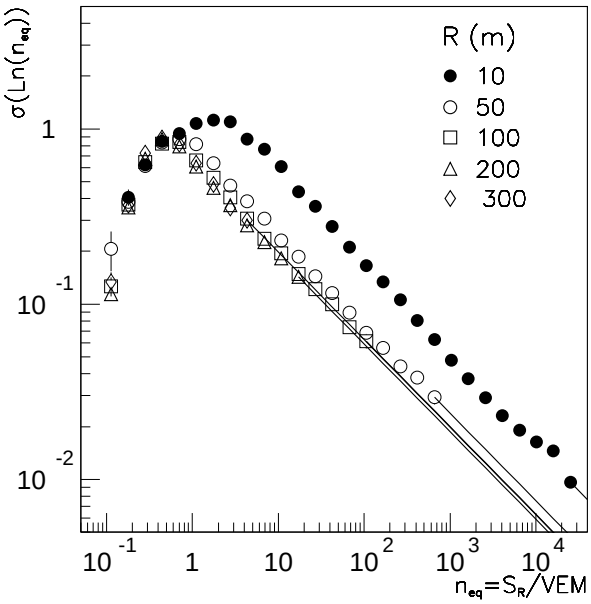

Fig. 13. Fluctuation of tank for different radii at photoelectron threshold $S_{\min} = 20$ (symbols). The lines are $1/\sqrt{n_{eq}}$ extrapolations normalized at the last (right) computed bins.

REFERENCES

[1] Fabian Kislat et al., Proc. 31^{st} ICRC, Lodz (2009).

[2] A.P. Garyaka, R.M. Martirosov, S.V. Ter-Antonyan et al., J. Phys.G: Nucl. and Part. Phys., **35** 2008, 115201 / arXiv:0808.1421 [astro-ph] (2008).

[3] A.P. Garyaka, R.M. Martirosov, S.V. Ter-Antonyan et al., Astropart. Phys. **28** (2007) 169. /arXiv:0704.3200 [astro-ph] (2007).

[4] J.M. Clem, P. Niessen, S. Stoyanov et al., Proc. 30 ICRC, 2007.